

Investigation of a cross-slot nanoantenna and extraordinary transmission

S. Rajbala, A. Srivastava, H.O. Pandey, V. Dinesh Kumar

Electronics and Communication Department, Indian Institute of Information Technology Design and Manufacturing (IIIT DM),
Dumna Airport Road, Jabalpur 482005, India
E-mail: dineshk@iiitdmj.ac.in

Published in Micro & Nano Letters; Received on 9th April 2012

Using finite integration technique, the authors investigate the properties of a cross-nanoslot formed in silver film, from the perspective of a plasmonic antenna, and examine the transmission of light through its periodic array. The cross-slot nanoantenna (CSNA) can enhance the intensity of near field by orders of magnitude, independent of polarisation of incident light, and emit omnidirectionally when excited by two identical sources of orthogonal polarisation operating in phase quadrature. An array of CSNA exhibit extraordinary transmission, which can be enhanced further by placing complementary cross-nanostripe array at an optimum position. To the authors' best knowledge, this is the first exploration of a cross-nanoslot as an antenna.

1. Introduction: An antenna acts as a progression device that converts guided electromagnetic (EM) waves into free space wave and vice versa. Recently, there has been a growing interest towards miniaturisation of RF antenna designs to optical frequency range for utilisation of their potential in the field of nanophotonics and plasmonics. It is believed that such nanoantennas could play a similar role in optical frequency range as played by conventional antennas in RFs [1–3]. Besides transmission and reception of optical signals these nanostructures may also find several other applications, such as biological imaging, efficient confinement and enhancement of light at nanoscale, efficient light coupling to nanoscale, guiding and redirecting light at nanoscale, near field and far field inter conversion, optical information processing at nanoscale, nanolight emitting devices/sources, nonlinear medium as an optical switch, solar cells, for realisation of metamaterials, etc. [4–9]. Thus, plasmonic nanoantennae may have much broader applications as compared with their RF counterparts and this urges for the exploration and design of novel antennas in optical frequencies. In this context, we can borrow ideas from highly developed RF antenna designs [10, 11] to produce more sophisticated optical antennas.

In this Letter, we investigate the EM properties of a cross-nanoslot from the viewpoint of antenna and study optical transmission through its periodic array. The cross-slot nanoantenna (CSNA) is formed by extending the feedgap of the recently proposed slot nanoantenna (SNA) [12], so as to form another slot orthogonal to the former. The structures of SNA and CSNA formed in a silver film on a silica substrate are shown in Figs. 1*a* and *b*, respectively. Using CST Microwave Studio (MWS), which is a commercial 3D EM simulator based on finite integration technique [13], first we investigate the spectral response of CSNA and observe that it can enhance intensity of near field by orders of magnitude, independent of polarisation. Secondly, we calculate the far field emission for various angles of polarisation of incident light. It is found that the azimuthal pattern of CSNA maintains the shape but rotates with the polarisation angle. The emission from CSNA is omnidirectional when operated in turnstile mode [10, 11], which draws useful analogies between classical EMs and nanophotonics. Thirdly, we investigate the effect of various geometrical parameters of CSNA on its spectral response.

Next, we study the extraordinary transmission (EOT) of light [14–16] from the periodic array of CSNA formed in a silver film of thickness 400 nm. The peak positions of transmission spectrum coincide with the peaks of near field intensity calculated at the centre of nanoslots. We demonstrate that the EOT can be enhanced further by placing an array of cross-nanostripes in alignment with the array of cross-nanoslots, directly above them, at an optimum distance [17]. The enhancement of transmission is attributed to the increased localisation of surface plasmon caused by the nanostripe

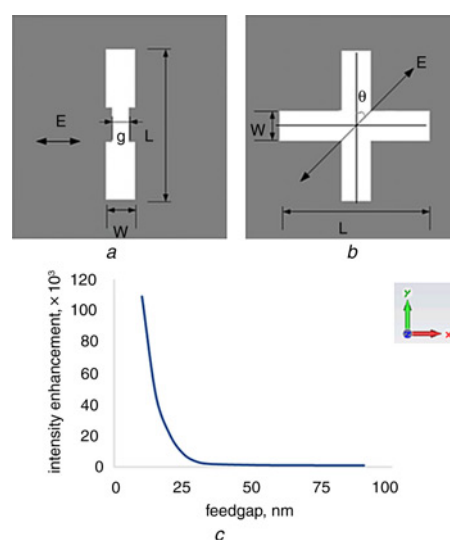


Figure 1 Characterisation of SNA

a SNA formed in a silver film of dimension $800 \times 800 \times 10$ nm. Slot length $L = 200$ nm, width $W = 40$ nm, feedgap $g = 10$ nm
b CSNA consisting of two orthogonal slots of SNA
c Variation of resonant intensity enhancement of SNA with feedgap dimension

near the cross-nanoslots. Finally, we examine the effect of polarisation of incident light on the EOT and observe that it is independent of polarisation.

Since the periodic array of cross-nanoslots is equivalent to an antenna array whose emission could be controlled by interspacing of the nanoslots and this will also control the EOT [14–16]. We speculate that for some specific periodicity, the CSNA array in a metal film could give rise to focused EOT. We believe that this is the first investigations of cross-nanoslots as antenna and the enhancement of EOT by complementary structures, which may be useful in the study of light–matter interaction and photonic devices such as optical nonlinear switch, etc. [18].

2. Simulation procedure: The SNA consists of a single slot of dimension 200×40 nm with a centre feedgap $g = 10$ nm cutout in a silver film of dimension $800 \times 800 \times 10$ nm on a silica substrate as shown in Fig. 1*a*. The CSNA consists of two identical orthogonal nanoslots each of dimension 200×40 nm formed in the silver film as shown in Fig. 1*b*. The structures are illuminated normally by broadband plane wave sources and open boundary conditions are imposed on the computational boundaries. The dielectric

function of silver, used by the software, has been derived by fitting a Drude model, into the experimental data provided by Johnson and Christy [19]

$$\varepsilon(\omega) = 1 - \frac{\omega_p^2}{\omega(\omega + j\omega_c)}$$

where ω_p is the electron plasma frequency (1.37×10^{16} Hz) and ω_c is the scattering frequency (3.21×10^{13} Hz). Near and far field monitors are placed in the computational region to record the field distribution and radiation pattern at particular frequencies.

Before performing actual investigation, we validated our simulation procedure against published results on near field enhancement and other EM properties of slot and cross dipole nanoantennae [3, 12, 20]. We also verified the experimental results of optical transmission through gold film of thickness 250 nm perforated with array of holes of diameter 200 nm and periodicity 600 nm on a quartz substrate. Strong transmission peak was found at 957 nm, which is in very close agreement with the published result [14].

2.1. Near field enhancement: The SNA is excited with X-polarised source, its resonant frequency is found to be 258 THz and the intensity enhancement of near field in the feedgap ($g = 10$ nm) is nearly five orders of magnitude larger. As the feedgap is increased from $g = 10$ nm the field intensity falls rapidly until $g = 20$ nm and rather less slowly beyond $g = 30$ nm as observed from Fig. 1c. When the feedgap becomes equal to the slot length 200 nm, it forms CSNA for which the intensity enhancement is still three orders of magnitude higher than the incident field, although in Fig. 1c variation of feedgap has been shown up to 90 nm only. The enhancement of near field by the nanoantenna is the consequence of giant buildup of charges of opposite polarity, because of excitation of localised surface plasmon (LSP) at the ends of the feedgap [7, 12].

We examine the effect of polarisation of incident field on the EM response of CSNA. The polarisation angle ' θ ' is varied from 0° to 90° in steps of 15° and the intensity spectra is calculated by placing probes at the centre of feedgap. It is evident from Fig. 2a that the resonant frequency remains the same at 258 THz for various polarisation angles; however, the intensity enhancement is insensitive to polarisation angle. This is so because, as the angular difference of polarisation from one slot increases it decreases with respect to the other; hence the resultant enhancement of field, being the vector sum of the two, remains unchanged for any polarisation angle. Mathematically we can express this as follows: For a given

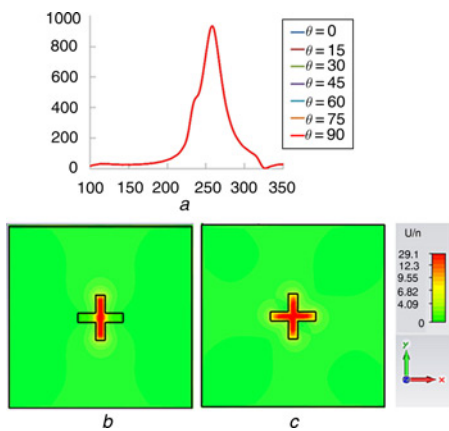


Figure 2 Effect of polarisation

a Spectral response of CSNA is independent of polarisation angle θ of excitation source field
b and c Depicting electric field distribution in the centre plane (XY) of the CNSA for polarisation angles $\theta = 90^\circ$ and 45° , respectively

polarisation angle θ the electric field of incident light at any frequency f can be resolved into two orthogonal components $E_0(f) \sin \theta$ and $E_0(f) \cos \theta$ exciting the vertical and horizontal slots respectively as shown in Fig. 1b. The enhancement of near field intensity by a slot is proportional to the intensity of incident field component normal to slot length [12]. The intensity of incident field components perpendicular to the two slots are $I_x(\theta, f) = E_0^2(f) \sin^2 \theta$ and $I_y(\theta, f) = E_0^2(f) \cos^2 \theta$. Thus, the resultant intensity enhancement because of the CSNA $\propto I_x(\theta, f) + I_y(\theta, f) = E_0^2(f) \sin^2 \theta + E_0^2(f) \cos^2 \theta = E_0^2(f)$. Clearly this is independent of polarisation of incident wave in the XY plane.

The intensity distribution of CSNA, at resonance, in its centre plane are plotted for polarisation angles $\theta = 90^\circ$ and 45° in Figs. 2b and c, respectively. It is found that for $\theta = 90^\circ$ only vertical slot is excited, whereas for $\theta = 45^\circ$ both the slots are excited.

2.2. Far field emission: The far field patterns of CSNA calculated, in its plane, for various polarisation angles are shown in Fig. 3a. The azimuthal pattern is bidirectional, having nulls in the direction of polarisation as expected. Since the structure is comprised of two identical orthogonal slots, the far field pattern maintains the shape but rotates with the polarisation angle [20].

In RF domain, turnstile antenna is a set of two dipole antennas aligned at right angles to each other and fed 90° degrees out-of-phase [10, 11]. Here, we operate the CSNA by two orthogonal linearly polarised sources and examine its response as a function of phase difference ' β ' between the two excitations. The azimuthal pattern is shown in Fig. 3b. It is seen that for $\beta = 0^\circ$ the pattern is bidirectional inclined at an angle of 45° because of the fact that the two sources, is equivalent to a single source with polarisation angle 45° . As β is increase from 0° to 90° , pattern gradually transforms into a near-circular form. Thus, the emission from CSNA operating in turnstile mode is found to be omnidirectional as seen from 3D radiation plot in Fig. 3c. To examine the polarisation of emitted radiation, we place a tiny line probe parallel to surface at distance 800 nm on its axis from the centre. It is found that the intensity recorded by the probe does not change as this is rotated about the Z-axis. This indicates that the radiation from CSNA operating in turnstile mode is circularly polarised [20].

2.3. Dependence on geometrical parameters: We examine the effect of various geometrical parameters of CSNA on its performance. First,

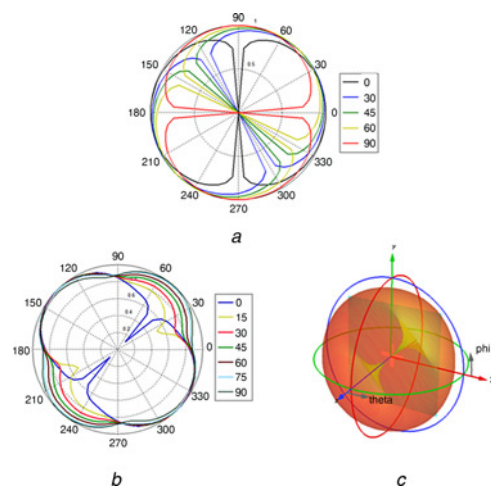


Figure 3 Far field emission of CSNA

a Azimuthal pattern of CSNA is bidirectional and rotates with polarisation angle θ maintaining its shape
b Radiation pattern of CSNA, operating in turnstile mode, gradually evolves from bidirectional to omnidirectional as the phase difference between the sources increases from $\beta = 0^\circ$ to 90°
c 3D emission pattern in turnstile operation of CSNA for $\beta = 90^\circ$

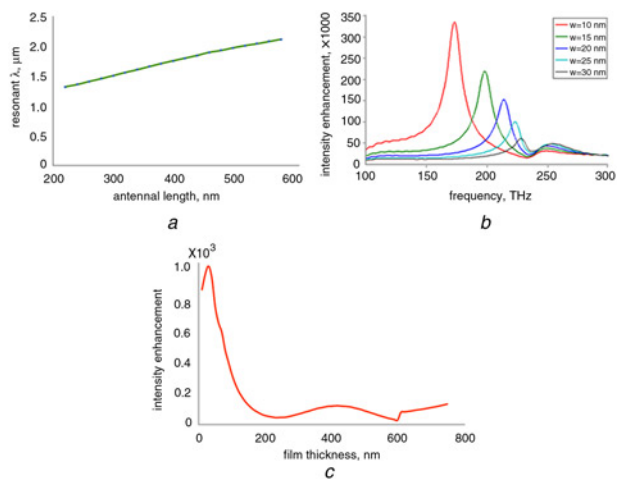


Figure 4 Dependence on geometrical parameters

a Resonant wavelength of CNSA varies linearly with its slot length
b Resonant frequency increases and sharpness of resonance decreases with increasing width W of slot
c Resonant intensity enhancement at the center of CSNA is very sensitive to film thickness for smaller thickness and varies nearly periodically when thickness is large

length of the slots is varied from 200 to 600 nm and the corresponding resonant wavelength is calculated. It is found that with increasing slot length L the resonant wavelength λ increases as shown in Fig. 4a, the variation is almost linear following equation $\lambda = 2.25L + 0.87$ (μm). This behaviour is similar to RF slot antennas for which resonant wavelength corresponding to fundamental mode is twice of its slot length $\lambda = 2L$ [11]. The resonant wavelength of CSNA, however, is found slightly greater than twice the slot length; this difference might be because of plasmonic excitation [21]. Next, width of the slots is varied from 20 to 70 nm and the spectral response of near field is calculated, the result is shown in Fig. 4b. It is observed that with increasing width W of slots, the resonant frequency of CSNA increases, but sharpness of resonance decreases. This happens because resonance of the structure depends on aspect ratio of slots L/W . Smaller the aspect ratio, smaller the resonant wavelength and hence higher the frequency. The sharpness of resonance decreases because of the same reason. Thus width of the CSNA plays an important role in near field enhancement, smaller the width more the enhancement of field intensity. Finally, thickness of the silver film is increased from 10 to 800 nm; keeping other parameters constant and its spectral responses are calculated by a probe at its centre. The dependence of intensity enhancement at resonance as a function of film thickness is plotted in Fig. 4c. For film thickness smaller than the skin depth (25 nm approximately), the localised surface plasmons generated at its top surface couples with the bottom surface plasmons [12]. The evanescent field of plasmonic mode generated at top surface extends into the metal and encounters a medium change at the bottom surface, thus making the resonance more sensitive to film thickness.

However for thickness greater than the skin depth, the excited plasmonic mode of top surface is not influenced by that of the bottom surface and hence the intensity becomes less sensitive to film thickness. For larger thickness of film, the intensity varies nearly periodically because of cavity effect of slot [17], as shown in Fig. 4c.

3. Extraordinary transmission: In this Section, we investigate the transmission from an array of CSNA, of dimension $L = 200$ nm, $W = 40$ nm, formed in silver film as shown in Fig. 5a and subsequently use an effective approach to enhance the EOT. We have introduced an array of silver cross-nanostripes over the nanoslots, as shown in Fig. 5b, where each nanostripe works as a cavity antenna [17]. At first glance, it may seem that the nanostrip is

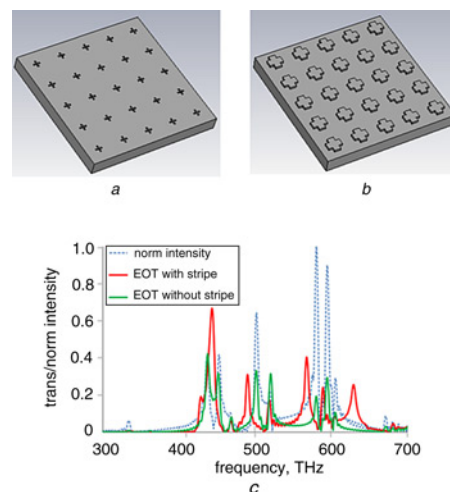


Figure 5 Characterisation of CSNA and transmission spectra

a Square array of CSNA of dimension 200×40 nm in silver film of thickness 400 nm, periodicity is $a_0 = 800$ nm
b Array of cross-nanostripes ($420 \times 190 \times 65$ nm) of silver placed 25 nm above the top surface of CSNA array
c Spectra of normalised intensity at centre of CSNA (blue dotted), EOT with (red) and without (green) array of nanostripes

blocking the incident light; however through the formation of nanocavity antenna, the nanostripes assist to couple more light into LSP of the CSNA, thus enhancing the EOT.

In the present investigation, we consider film thickness $t = 400$ nm, much larger than the skin depth as for this thickness intensity enhancement at the centre of CSNA is maximum as shown in Fig. 4c. The periodicity of CSNA is $a_0 = 800$ nm and the dimension of cross-nanostripes used is $420 \times 190 \times 65$ nm; these are placed 25 nm above the film surface.

Using CST MWS, first we calculate the transmission spectrum of an infinite array, in the frequency range 200–700 THz, when illuminated normally by planewave polarised along $\theta = 0^\circ$; this is shown (green) in Fig. 5c. The transmission is extraordinary nearly 41% corresponding to the first peak at 437 THz. All peak positions are almost in accordance with the formula [16] for normal incidence given as:

$$\lambda_{\max}(i, j) = \frac{a_0}{\sqrt{i^2 + j^2}} \sqrt{\frac{\epsilon_s \epsilon_m}{\epsilon_s + \epsilon_m}}$$

We also calculate the intensity of localised fields at the centre of the cross-nanoslots as a function of frequency. The normalised intensity spectrum is shown by dotted blue line. It is interesting to see that the transmission peaks coincide with the peaks of intensity spectrum. This indicates that the high transmission is the result of localised fields in the nanoslot caused by plasmonic excitation [14, 15].

Next we calculate the transmission of periodic structure with array of cross-nanostripes placed above the film, this is shown by red line. Interestingly the normalised transmission corresponding to first peak at 442 THz is increased to 65%. The slight shift in peak positions might be because of the influence of nanostripes on the resonance of nanoslots. The reason for the enhancement of EOT in presence of the nanostripes will be clear if we look at Figs. 6a and c, depicting the distribution of tangential component of magnetic field on the surface of CNSA, in the unit cell of periodic structure, with and without the nanostripes. It is clear that the magnetic field is more intensely localised near the nanoslots in presence of the nanostripes, causing larger surface current to pass through them, and hence enhanced EOT. This fact can also be observed from the field distribution in the cross section (the

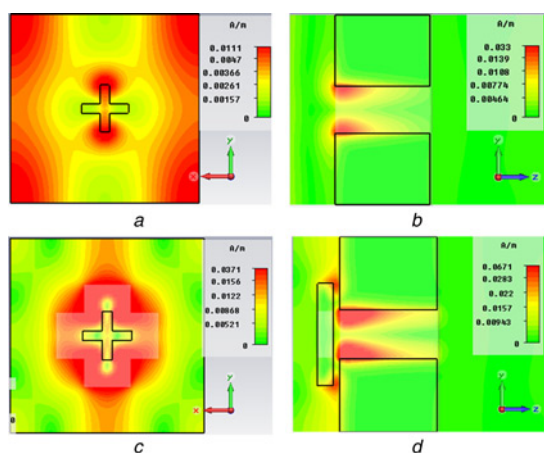


Figure 6 Enhancement of EOT

a Distribution of tangential component of magnetic field H in the unit cell of array
 c Localisation is stronger around CSNA in presence of cross-nanostripes
 b and d Corresponding distribution shown in the cross-section (YZ) of nanoslots
 Incident field is X polarised ($\theta = 900$)

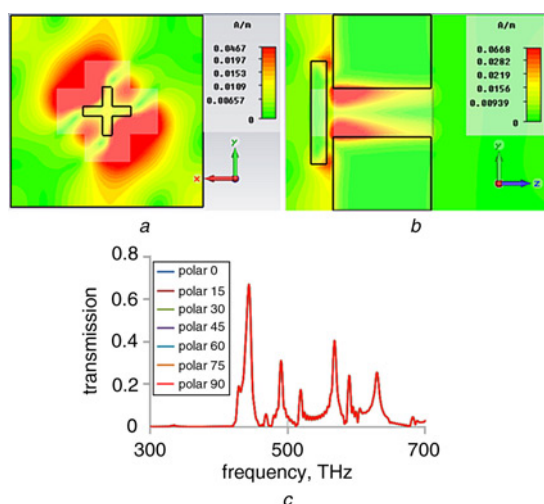


Figure 7 EOT independent of polarisation of incident light

a Tangential magnetic field distribution in the unit cell for polarisation angle $\theta = 450$; surface plane (XY)
 b Cross-section (YZ)
 c EOT from CSNA array in presence of array of cross-nanostripes is independent of polarisation angle θ

YZ plane) of nanoslots shown in Figs. 6b and d. As seen, the intensity is nearly twice in presence of the nanostripes as compared to the case when they are not present. Thus the presence of nanostripes help in coupling more light into plasmonic mode, resulting in enhanced transmission.

The EOT is found to be independent of polarisation of incident light as shown in Fig. 7c. The polarisation is varied from $\theta = 0^\circ$ to 90° in steps of 15° and normalised transmission is found to be the same in all cases. The magnetic field distribution is plotted for polarisation angle $\theta = 45^\circ$, in XY and YZ planes, in Figs. 7a and b, respectively. Evidently, the distribution of field intensity in slot cross-section is the same as compared to the case when $\theta = 0^\circ$ as shown in Fig. 6d. Since EOT is the result of LSP in the nanoslots, this explains why it is independent of incident polarisation.

4. Conclusions: We have studied the field enhancement and radiation properties of cross-nanolots formed in a silver film from the

perspective of plasmonic antenna, we call this CSNA. The structure can enhance the intensity of incident field by orders of magnitude, independent of polarisation, and emit omnidirectionally when excited by dual sources with orthogonal polarisation operating in phase quadrature. An array of CSNA in metal film gives rise to EOT nearly 41% at the fundamental peak of 437 THz. The transmission peaks for various orders coincide with the peaks of intensity spectra calculated at the centre-of-cross nanoslots. The inclusion of cross-nanostripe in the array, placed at optimum distance above the CSNA enhances the EOT at fundamental peak. It will be easy to fabricate CSNA and its emission is free from background radiation, these are the added advantages of CSNA as compared to other plasmonic nanoantennae.

5 References

- [1] Alu A., Engheta N.: 'Tuning the scattering response of optical nanoantennae with nanocircuit loads', *Nat. Photonics*, 2008, **2**, pp. 307–310
- [2] Fischer H., Martin O.J.F.: 'Engineering the optical response of plasmonic nanoantennas', *Opt. Express*, 2008, **16**, (12), pp. 9144–9154
- [3] Muhlshlegel P., Eisler H.J., Martin O.J.F., Hecht B., Pohl D.W.: 'Resonant optical antennas', *Science*, 2005, **308**, pp. 1607–1609
- [4] Cubukcu E., Kort E.A., Crozier K.B., Capasso F.: 'Plasmonic laser antenna', *Appl. Phys. Lett.*, 2006, **89**, (9), pp. 093120–093123
- [5] Brongersma M.L.: 'Engineering optical nanoantennae', *Nat. Photonics*, 2008, **2**, pp. 270–272
- [6] Bakker R.M., Yuan H.-K., Lui Z., ET AL.: 'Enhanced localized fluorescence in plasmonic nanoantennae', *Appl. Phys. Lett.*, 2008, **92**, pp. 043101–043103
- [7] Yu N., Cubukcu E., Diehl L., ET AL.: 'Bowtie plasmonic quantum cascade laser antenna', *Opt. Express*, 2007, **15**, p. 13272
- [8] Jiasen Z., Jing Yang X.W., Gong Q.: 'Electric field enhancing properties of the V-shaped optical resonant antennas', *Opt. Express*, 2007, **15**, (25), pp. 16852–16859
- [9] Imhof C., Zengerle R.: 'Materials science and processing', *Appl. Phys. A*, 2009, **94**, p. 45
- [10] Balanis C.A.: 'Modern antenna handbook' (Wiley-Interscience, 2008)
- [11] Karuss J.D.: 'Antennas' (McGraw-Hill Book Company, New York, 1988, 2nd edn.)
- [12] Dinesh Kumar V., Asakawa K.: 'Investigation of a slot nanoantenna in optical frequency range', *Photonics Nanostruct.: Fundam. Appl.*, 2009, **7**, pp. 161–168
- [13] CST Microwave Studio, 3D EM simulator, <https://www.cst.com/>
- [14] Krishnan A., Thio T., Kim J., ET AL.: 'Evanescantly coupled resonance in surface Plasmon enhanced transmission', *Opt. Commun.*, 2001, **200**, pp. 1–7
- [15] Genet C., Ebbesen T.W.: 'Light in tiny holes', *Nature*, 2007, **445**, pp. 39–46
- [16] Barnes W.L., Dereux A., Ebbesen T.W.: 'Surface plasmon subwavelength optics', *Nature*, 2003, **424**, pp. 824–830
- [17] Cui Y., He S.: 'Enhancing extraordinary transmission of light through a metallic nanoslit with a naocavity antenna', *Opt. Lett.*, 2009, **34**, (1), pp. 16–18
- [18] Asakawa K., Sugimoto Y., Watanabe Y., ET AL.: 'Photonic crystal and quantum dot technologies for all-optical switch and logic device', *New J. Phys.*, 2006, **8**, pp. 1–26
- [19] Johnson P.B., Christy R.W.: 'Optical constants of the noble metals', *Phys. Rev. B*, 1972, **6**, (12), pp. 4370–4379
- [20] Kumar D.V., Bhardwaj A., Mishra D.: 'Investigation of a turnstile nanoantenna', *Micro Nano Lett.*, 2011, **6**, (2), pp. 94–97
- [21] Novotny L.: 'Effective wavelength scaling for optical antennas', *Phys. Rev. Lett.*, 2007, **98**, (26), pp. 266802–266805